Insights into the Deposition of Nanometer-Thick Nickel Oxide Films by Amino Acid Chelated Complex for Electrochromic Smart Windows

We present a systematic investigation of nickel oxide (NiO_x) prepared from Ni(II) complexes with monodentate β-alanine ligands or with bidentate L-alanine ligands and their potential for use in electrochromic materials. Our main findings were that although a similar oxidation state of NiO_x was generated using Ni(II)-L-alanine or Ni(II)-β-alanine complexes, the Ni(II)-L-alanine complex led to the deposition of a homogenous film with a small grain size. We ascribed the different grain sizes of the samples to the differences in the dissociations of these ligands during electrodeposition. Furthermore, the sample with a small grain size exhibited a good cycling stability and high coloration efficiency compared to the other sample.

The use of coordination complexes as metal precursors for electrodeposition of transition metal oxide nanostructures provides a novel approach for fabricating unique nanostructures [1]. However, many unanswered questions remain regarding the effect of the complex structure on the formation of transition metal oxide nanostructures. In a previous work, we reported a systematic investigation of nickel oxide (NiO_x) films prepared from Ni(II) complexes with bidentate L-alanine ligands (NiO_x-LAla) or with monodentate β-alanine ligands (NiO_x-βAla) and their potential for use in electrochromic (EC) windows [2]. **Figure 1(A)** shows the UV-vis absorption spectra for the samples electrodeposited for 2 h. In contrast to NiO_x-βAla, the absorption intensities for NiO_x-LAla were considerably higher, suggesting that the film thickness, or growth rate, of the samples was different in these solutions.

The structures of NiO_x-LAla and NiO_x-βAla were investigated using X-ray absorption fine structure (XAFS) spectroscopy. In the spectra of *in situ* Ni K-edge X-ray absorption near-edge structure (XANES), the edge positions of NiO_x-LAla and NiO_x-βAla matched that of γ-NiOOH [**Fig. 1(B)**]. Based on a calibration of the reference compounds, the average nickel valence of the samples was estimated to be ca. +3.4. A comparison of the Fourier transforms (FT) of the extended X-ray absorption fine structure (EXAFS) spectra showed that the peak positions of the first (Ni–O) and second (Ni–Ni) coordination shells for NiO_x-LAla and NiO_x-βAla were similar to those of γ-NiOOH. These observations demonstrated that the local structures of both samples consisted of edge-sharing NiO_6 octahedra [**Fig. 1(B)**]. Moreover, the FT EXAFS spectra showed that the peak intensities of NiO_x-LAla were weaker than those of NiO_x-βAla, suggesting a smaller nanocluster size for NiO_x-LAla. Atomic force microscopy (AFM) was used to obtain more direct information regarding the film topography. AFM images of NiO_x-LAla and NiO_x-βAla showed that the samples consisted of closely stacked grains [**Fig. 1(C)**]. In contrast to NiO_x-βAla, NiO_x-LAla had a small grain size and low root mean square surface roughness. Overall, the Ni(II)-L-alanine complex led to the deposition of a homogenous film with small grain/cluster size compared to the Ni(II)-β-alanine complex.

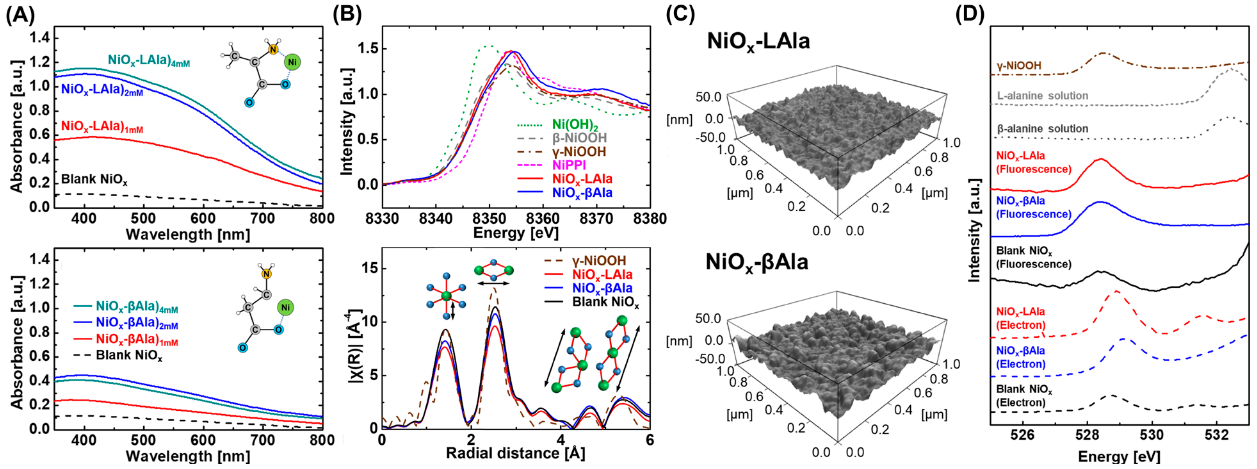

Figure 1: (A) UV-vis absorption spectra, **(B)** XANES spectra and FT EXAFS spectra, **(C)** AFM images, and **(D)** O K-edge XAFS spectra of NiO_x samples. Reproduced with permission from Ref. [2]. Copyright 2020, American Chemical Society.

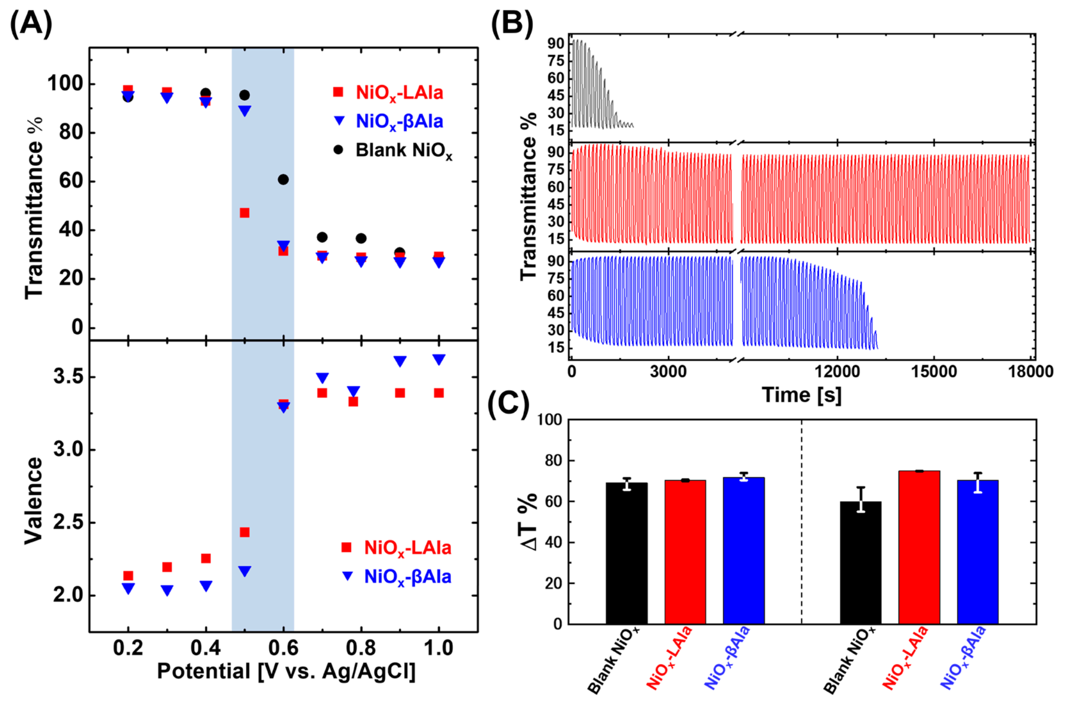

Figure 2: (A) In situ transmittance change and the corresponding Ni valence change, **(B)** switching response curves (NiO_x-LAla in red, NiO_x-βAla in blue), and **(C)** maximum optical modulation measured at 25 (left) and 50 °C (right) of NiO_x samples. Reproduced with permission from Ref. [2]. Copyright 2020, American Chemical Society.

To further understand the effect of alanine on the structure of electrodeposited NiO_x, the fluorescence and electron yield methods were used to obtain the O K-edge XAFS spectra of NiO_x-LAla and NiO_x-βAla. **Figure 1(D)** shows the O K-edge XAFS spectra obtained in both modes, where the γ-NiOOH peak was positioned at ca. 528 eV for each sample. In the electron yield spectra, the L-alanine peak around 532 eV was observed for NiO_x-LAla but the β-alanine peak near 532 eV was not observed for NiO_x-βAla. Considering that electron yield detection is surface sensitive and the escape path of photons from X-ray fluorescence is in the range of a few micrometers [3], we believe that L-alanine was present only near the surface of NiO_x-LAla but not in the bulk of the sample. By contrast, β-alanine was absent from both the surface of NiO_x-βAla and from the bulk of the sample. We assume that L-alanine and β-alanine molecules were gradually cleaved from Ni ions upon the electrodeposition of NiO_x, and β-alanine was especially liable to dissociate because it was a monodentate ligand. This constituted a possible reason for the different grain/cluster sizes of NiO_x-LAla and NiO_x-βAla.

Figure 2(A) shows the *in situ* transmittance change and the corresponding Ni valence change for NiO_x-LAla and NiO_x-βAla measured at an optical wavelength of 400 nm in response to applied potentials of 0.2 to 1.0 V. When the coloring potential was below 0.5 V, both samples showed marginal differences in their optical transmittance. At a potential of 0.5 V, there was an obvious decrease in optical transmittance from 98 to 47% for NiO_x-LAla. This was accompanied by a change in Ni valence from 2.1 to 2.4, indicating that NiO_x-LAla was more oxidized than NiO_x-βAla. Comparing coloration efficiency and cycling stability for both samples, NiO_x-LAla exhibited a high coloration efficiency of 78.4 cm^2/C and nearly 100% retention of the initial optical modulation value even after 150 cycles [**Fig. 2(B)**]. Moreover, NiO_x-LAla showed an excellent thermal stability compared to NiO_x-βAla. There was almost no change in optical modulation for NiO_x-LAla with an increase in the ambient temperature from 25 to 50 °C [**Fig. 2(C)**]. However, the optical modulation of NiO_x-βAla decreased to 64% because it could not be bleached completely. Overall, our findings provide insights into the mechanisms through which amino acid chelated complexes could be used to deposit transition metal oxide nanostructures with favorable EC characteristics.

REFERENCES

[1] M. Yoshida, S. Onishi, Y. Mitsutomi, F. Yamamoto, M. Nagasaka, H. Yuzawa, N. Kosugi and H. Kondoh, *J. Phys. Chem. C* **121**, 255 (2017).
[2] K. H. Wang, H. Ikeuchi, M. Yoshida, T. Miura, I. P. Liu, G. Watanabe, S. Cui and T. Kawai, *ACS Appl. Nano Mater.* **3**, 9528 (2020).
[3] M. Honda, Y. Baba, I. Shimoyama and T. Sekiguchi, *Rev. Sci. Instrum.* **86**, 035103 (2015).

BEAMLINES

BL-7A, BL-9A and BL-16A.

K. H. Wang[1], M. Yoshida[2] and T. Kawai[1] ([1]Tokyo Univ. of Science, [2]Univ. of Yamaguchi)